DIURNAL CYCLE OF TROPICAL DEEP CONVECTION AND ANVIL CLOUDS: GLOBAL DISTRIBUTION USING 6 YEARS OF TRMM RADAR AND IR DATA

Chuntao Liu[*] and Ed Zipser
Department of Meteorology, University of Utah

1. INTRODUCTION

Before the launch of the TRMM satellite in late 1997, most studies of the diurnal cycle of tropical convective clouds used IR data only [e.g., Fu et al., 1990; Janowiak et al., 1994; Garreaud and Wallace, 1997]. A typical metric would be the area covered by clouds whose outgoing long wave radiation (or IR brightness temperature) was less than some specified value [Hall and Vonder Haar, 1999; Yang and Slingo, 2001]. The area covered by cold cloud was often used as a proxy for coverage of deep or intense convection, or for rainfall. The association is a logical one, because high cold clouds are usually anvil clouds produced directly by deep precipitating convective clouds. Using the Precipitation Radar (PR) and the Visible and Infrared Scanner (VIRS) on the TRMM satellite, it is possible now to view the high cold anvil clouds, and at the same time the structure of the precipitating convection, and do so globally [Liu et al, 2006]. This study combines the PR and VIRS measurements, focusing on the diurnal cycle of anvil clouds identified by VIRS, the diurnal cycle of deep convection observed by the PR, their similarities and their differences.

2. DATA AND METHOD

After matching 7 years (1998-2004) of TRMM PR and VIRS measurements within the PR swath, the Precipitation Features (PFs) and Cold Cloud Features (CCFs) are identified independently. The former are defined by contiguous PR raining areas; the latter by contiguous areas of cold VIRS 11 micrometer brightness temperature (T_{B11}) colder than 235 K. An example of a CCF is shown in Figure 1. For each CCF, the T_{B11} area, number of contiguous raining areas (PFs), area of $T_{B11} < 210$ K, area of PR 20 dBZ reaching 14 km, flash counts and volumetric rain are calculated. Due to instrument problems in September and October 2002 and the satellite orbit boost in August 2001, some VIRS measurements are missing or not reliable. For this reason, only 1998-2001 and 2003-2004, a total of 6 years CCFs, with knowledge of the Aug 2001 data replaced by

* *Corresponding author address*: Chuntao Liu. Univ. of Utah, Dept. of Meteorology, Salt Lake City, UT, 84112; e-mail: liuct@met.utah.edu.
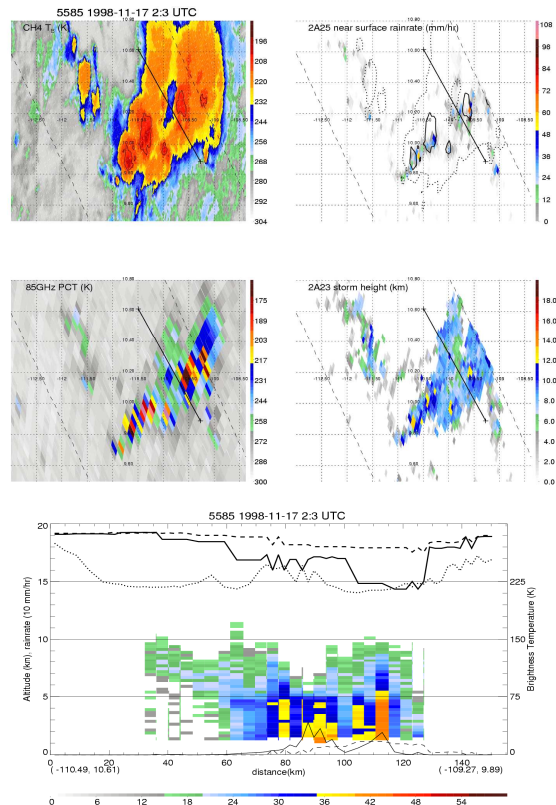
Figure 1. An example of TRMM observed CCF in Nov, 17, 1998. Top panels show T_{B11}, 2A25 near surface rain, 85 GHz PCT, and storm height detected from PR profiles. Contours of T_{B11} 210 K (solid line) and 235 K (dash line) are overlapped with near surface rain in top right panel. Bottom panel shows the vertical cross section at the location of thick solid line on top panels. Lines in this panel represents 85 GHz PCT (thick solid), 37 GHz PCT (thick dash), T_{B11} (dot), 2A25 near surface rainfall rate (thin solid), and 2A12 surface rainfall rate (thin dash).

August 2002 data, will be discussed in this work.

Insufficient samples have been one big obstacle in the diurnal analysis [Negri et al., 2002]. There are now more than 4 million CCFs identified in this 6-year dataset. However, they are not evenly distributed (Figure 2). For this reason, diurnal analysis will only be applied to the specific regions (Figure 2) with large areas, and 10° x10^o grids with

more than 8000 samples (Figure 2).

In practice, three steps were performed to obtain the diurnal variation of convective intensity and cloud properties of CCFs. First, local times of CCFs are calculated from the CCFs's universal times and longitudes. Then, they are separated within 2 hour local time bins. Lastly, mean values, harmonic phases and amplitudes of area of 20 dBZ above 14 km, flash counts, area of cloud < 210 K, 235 K, and volumetric rain in each bin are calculated.
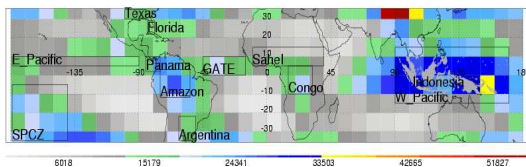
Figure 2. Distribution of sample populations and regions of interest.

3. RESULTS AND DISCUSSION

This section first shows the results of mean phase and amplitude of diurnal variation from harmonic analysis, then investigates the phase lags among the different variables, and lastly, discusses the diurnal variation of anvil clouds defined with non-raining 235 K area.

3.1 Mean, phase and amplitudes

Mean values of PF population, area of 20 dBZ reaching 14 km, area of $T_{B11} < 210$ K and 235 K, and volumetric rain from CCFs in 10°x10^{o} boxes are shown in Figure 3. Most PFs occurred over the west Pacific ocean, Indonesia and the Amazon Basin. But the most overshooting (20 dBZ reaching 14 km) occurred over land, especially over central Africa [Liu and Zipser, 2005]. The distributions of cold cloud areas ($T_{B11} < 210$ K, 235 K) show a similar pattern as volumetric rain: high values over the west Pacific, Amazon, and Congo. Diurnal variation amplitude of overshooting and very cold clouds ($T_{B11} < 210$ K) has much stronger diurnal variations than the PF population, "warmer" clouds ($T_{B11} < 210$ K) and precipitation (Figure 4). In general, diurnal variation amplitude over land is stronger than over ocean, which is consistent with past studies [e.g. Hall and Vonder Haar, 1999; Yand and Slingo, 2001; Tsakraklides and Evans, 2003, Nesbitt and Zipser, 2003]. Diurnal harmonic (S1) phase in Figure 5 shows a clear afternoon maximum of almost all variables over land, nocturnal maxima of overshooting and clouds

< 210 K over ocean, and morning maxima of population of PFs, 235 K clouds and volumetric rain. Clearly, there are numerous phase lags in the diurnal variations of the different variables.
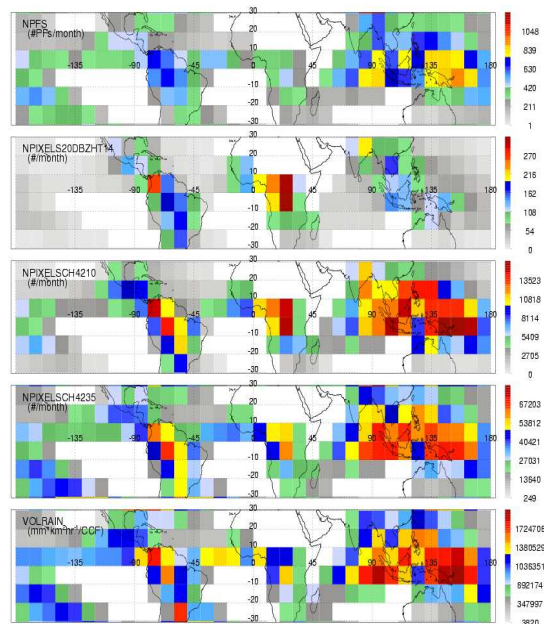
Figure 3. Monthly mean of PF population, area of 20 dBZ reaching 14 km, area of $T_{B11} < 210$ K and 235 K , and volumetric rain from CCFs in 10°x10^{o} boxes.
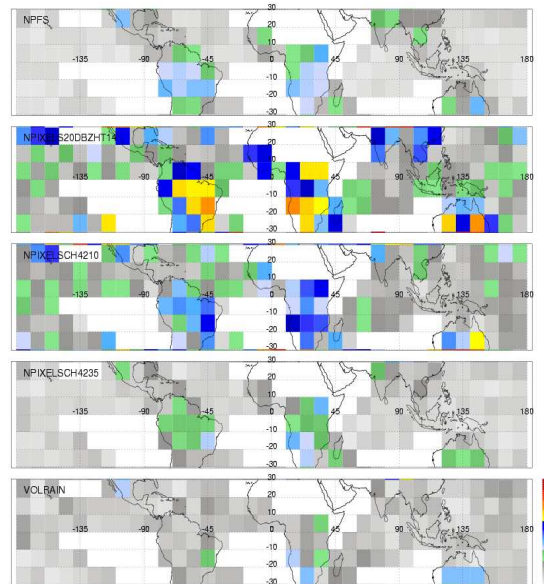
Figure 4. Diurnal variation amplitude of PF population, area of 20 dBZ reaching 14 km, area of $T_{B11} < 210$ K and 235 K, and volumetric rain from CCFs in 10°x10^{o} boxes.
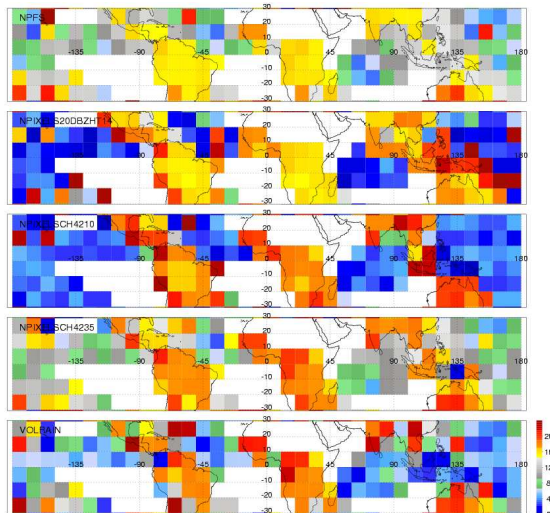
Figure 5. Diurnal variation phase (S1) of PF population, area of 20 dBZ reaching 14 km, area of T_{B11} < 210 K and 235 K, and volumetric rain from CCFs in 10^ox10^o boxes.

3.2 Phase lags

To investigate the phase lags shown in Figure 5, the same variables from 20^oS-20^oN land and oceanic CCFs are normalized hourly, and shown with S1 phases in Figure 6. Notice that S1 phases are not consistent with the maximum phases for all variables.
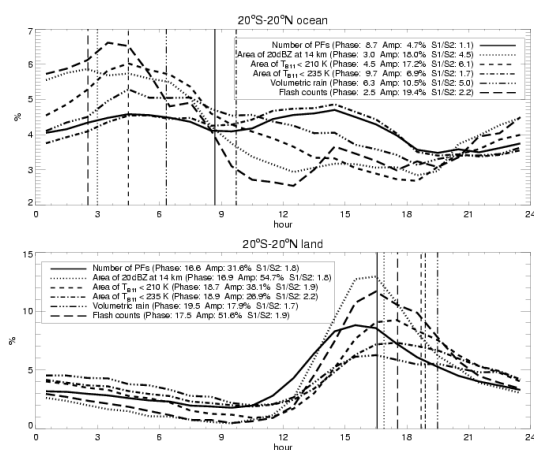
Figure 6. Diurnal variation of PF population, area of 20 dBZ reaching 14 km, area of T_{B11} < 210 K and 235 K , flash counts, and volumetric rain in 20^oS-20^oN CCFs. The vertical lines represent the location of the diurnal harmonic phase (S1).

Over land, S1 phases are found 0.5~1 hour later than the maximum phase. But they can still be used as fair indicators for the phase lags in different variables. First, the population of convective cells reaches its maximum in late afternoon, followed quickly by the development of deep intense convection (20 dBZ reaching 14 km). After gradual spreading of anvil clouds, the amount of 210 K and 235 K clouds increases to a maximum in 2-3 hours, followed by the most intense rainfall. This similar pattern can be found for different tropical land regions (Figure 7), although there are regional differences illustrated by earlier and shorter convection life cycles over the Amazon than those over the Congo and Indonesia. Convection over Indonesia has the latest and longest life cycle of the three tropical regions. Speculation is that relatively weaker convection over the Amazon [Nesbitt et al., 2000; Cecil et al., 2005] has a shorter life cycle.
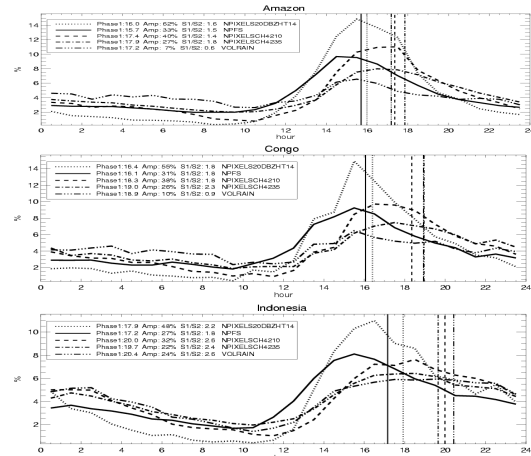
Figure 7. Similar to figure 6, but analyzed 2-hourly for CCFs over Amazon, Congo, and Indonesia.

Over oceans, S1 phases cannot indicate the phase lags among the diurnal variations of different variables because of the multiple modes in the variations (Figure 6). Overshooting, area of T_{B11} < 210 K, and flash counts show strong diurnal variation in contrast to the semi-diurnal variation of PF population and area of T_{B11} < 235 K. The similar semi-diurnal patterns over the east and west Pacific, and the north Atlantic in Figure 8 suggest that the early afternoon maxima is not just coastal effects. With less cloud (T_{B11} < 235 K) amount but more volumetric rain, the nocturnal cloud systems seem to produce more precipitation per area of clouds than afternoon clouds over oceans. With these results, an image of the life

cycle of oceanic convection diurnal variation can be achieved:

The highest population of convective cells is after midnight, followed by overshooting convection, which produces very cold clouds (< 210 K) with heavy precipitation in the early morning. (However, this is rarely accompanied by lightning according to Cecil et al. 2005). During the early afternoon, more convective cells appear under a larger area of 235 K clouds. These clouds have relative weaker convection (with rare overshooting radar echoes or clouds < 210 K), and produce less precipitation.
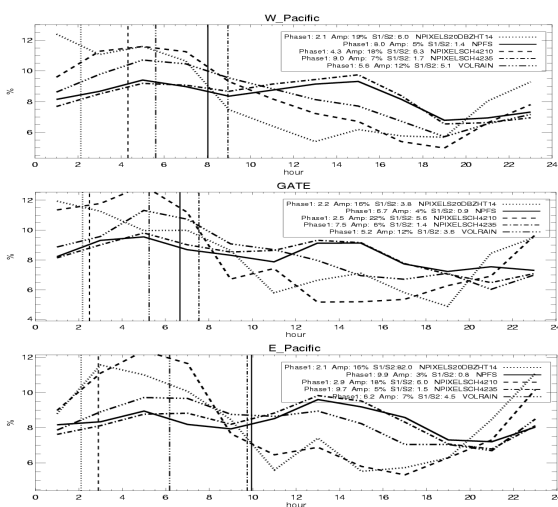
Figure 8. Similar to figure 6, but analyzed 2-hourly for CCFs over the west Pacific, the north Atlantic and the east Pacific.

3.3 Diurnal variation of anvil area

To understand better the low ratio of rain volume to other measured parameters of the early afternoon oceanic clouds, it is important to quantify the portion of these clouds without rain. For this purpose, anvil clouds are defined as the non-raining area of CCFs After accumulating the number of non-raining pixels inside CCFs in 4 hour bins within $10^{o} \times 10^{o}$ boxes, the diurnal variation of area of the anvil clouds is generated (Figure 9). The amount of anvil cloud over land reaches its maximum during the late afternoon and decreases till the next morning. Large amounts of anvil clouds are found over the west Pacific throughout the 24 hours. Hourly accumulated anvil size (Figure 10) confirmed the afternoon peak of anvil cloud amount over land. Amazon anvil cloud amount reaches its maximum earlier than that over Congo

and Indonesia. Over ocean, there are two modes with a similar pattern as the variation of 235 K cloud amounts in Figure 6. One reaches its maximum at early morning, and another one at early afternoon. More oceanic anvil clouds are found during the early afternoon than during the night.
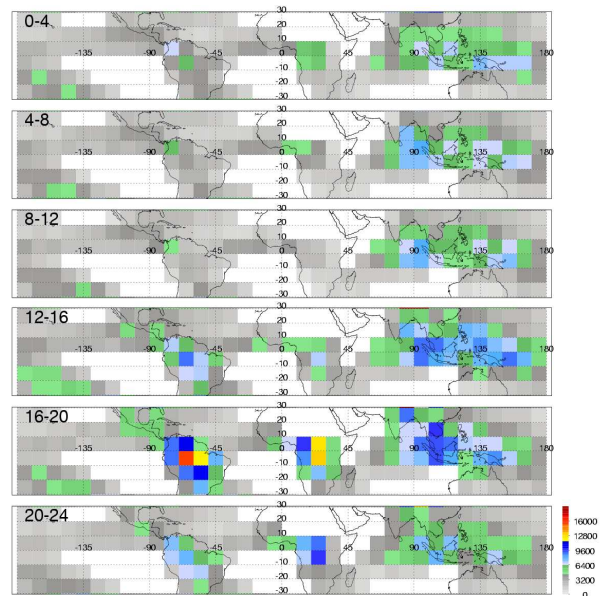
Figure 9. 4 hourly distribution of number TRMM observed pixels with anvil (non-raining) clouds in CCFs.
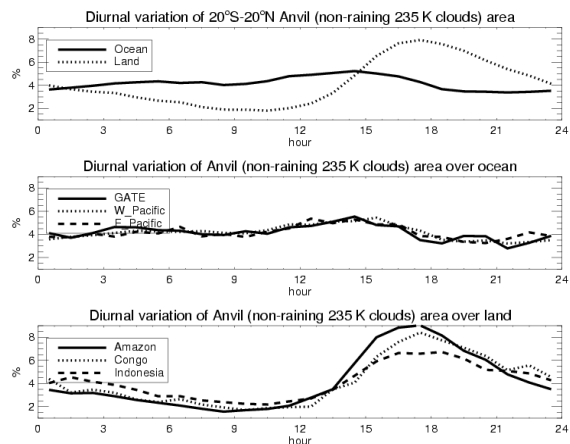
Figure 10. Diurnal variation of the anvil (non-raining) cloud amount over different regions.

4. SUMMARY

By defining CCFs from 6 years TRMM data, the mean, amplitude, and phase of diurnal variation of precipitation and convective intensity properties of

clouds colder than 235 K are shown. The composite life cycle of tropical deep convection is demonstrated by showing the time lags among the maximum phases of the diurnal cycle, differently defined. Over land, first we observe a peak in the population of PFs, dominated by small showers. Next in quick succession comes the peak in area of PFs reaching 14km, then CCFs area < 210 K, and finally CCFs area < 235 K and precipitation. Amazon CCFs has the earliest peaks and shortest life cycle. Over ocean, there are relative weak diurnal variations of 210 K cloud amount and semi-diurnal variations of population of PFs and the 235 K cloud amounts. Nocturnal oceanic clouds have stronger convection with overshooting and have relative higher ratios of precipitation to cloud amount than the early afternoon clouds, which have larger cloud coverage and relatively weaker convection.

REFERENCES

Cecil, D. J., S. J. Goodman, D. J. Boccippio, E. J. Zipser and S. W. Nesbitt, 2005: Three Years of TRMM Precipitation Features. Part I: Radar, Radiometric, and Lightning Characteristics, *Mon. Wea. Rev.* **133**, 543–566.

Fu, R., A. D. Del Genio, and W. B. Rossow, 1990: *J. Climate*, **3,** 1129-1152.

Garreaud, R. D., and J. M. Walac, 1997: The diurnal march of convective cloudiness over the Americas. *Mon. Wea. Rev.*, **125**, 3157-3171.

Hall, T. J., and T. H. Vonder Haar, 1999, The diurnal cycle of west Pacific deep convection and its relation to the spatial and temporal variation of tropical MCSs, *J. Atmos. Sci.*, **56**, 3401-3415.

Janowiak, J., P. A. Arkin, and M. Morrissey, 1994: An examination of the diurnal cycle in oceanic tropical rainfall using satellite and in situ data. *Mon. Wea. Rew.*, **122**, 2296-2311.

Liu, C., and E. Zipser, 2005: Global distribution of convection penetrating the tropical tropopause. *J.Geophys. Res.-Atm*, **110**, D23104, doi:10.1029/2005JD006063

Liu, C., E. Zipser, and S. Nesbitt, 2006: Global distribution of deep convection: why do Radar and IR images give different perspective? Manuscript submitted to *J. Climate*.

Negri, A. J., T. Bell, L. Xu, 2002: Sampling of the diurnal cycle of precipitation using TRMM. *J. Atmos. Ocean. Tech.*, **19**, 1333-1344.

Nesbitt, S. W., E. J. Zipser, and D. J. Cecil, 2000: A census of precipitation features in the tropics using TRMM: radar, ice scattering, and lightning observations. *J. Climate.*, **13**, 4087-4106.

Nesbitt, S. W., and E. J. Zipser, 2003: The diurnal cycle of rainfall and convective intensity according to tree years of TRMM measurements. *J. Climate,* **16**, 1456-1475.

Tsakraklides, G. and J. L. Evans, 2003: Global and regional diurnal variations of organized convection, *J. Climate*, **16**, 1562-1572.

Yang, G.-Y, and J. Slingo, 2001: The diurnal cycle in the tropics, *Mon. Wea. Rev.*, **129**, 784-801.